Journal of Cerebral Blood Flow & Metabolism (2010) 30, 1275–1287

www.jcbfm.com

Oxygen-sensitive outcomes and gene expression in acute ischemic stroke

Cameron Rink[1], Sashwati Roy[1], Mahmood Khan[2], Pavan Ananth[1], Periannan Kuppusamy[2], Chandan K Sen[1] and Savita Khanna[1]

[1]*Department of Surgery, The Ohio State University Medical Center, Columbus, Ohio, USA;* [2]*Department of Internal Medicine, The Ohio State University Medical Center, Columbus, Ohio, USA*

Acute ischemic stroke (AIS) results in focal deprivation of blood-borne factors, one of them being oxygen. The purpose of this study was two-fold: (1) to identify therapeutic conditions for supplemental oxygen in AIS and (2) to use transcriptome-wide screening toward uncovering oxygen-sensitive mechanisms. Transient MCAO in rodents was used to delineate the therapeutic potential of normobaric (NBO, 100% O_2, 1ATA) and hyperbaric oxygen (HBO, 100% O_2, 2ATA) during ischemia (iNBO, iHBO) and after reperfusion (rNBO, rHBO). Stroke lesion was quantified using 4.7 T MRI at 48 h. Supplemental oxygen during AIS significantly attenuated percent stroke hemisphere lesion volume as compared with that in room air (RA) controls, whereas identical treatment immediately after reperfusion exacerbated lesion volume (RA = 22.4 ± 1.8, iNBO = 9.9 ± 3.6, iHBO = 6.6 ± 4.8, rNBO = 29.8 ± 3.6, rHBO = 35.4 ± 7.6). iNBO and iHBO corrected penumbra tissue pO_2 during AIS as measured by EPR oxymetry. Unbiased query of oxygen-sensitive transcriptome in stroke-affected tissue identified 5,769 differentially expressed genes. Candidate genes were verified by real-time PCR using neurons laser-captured from the stroke-affected somatosensory cortex. Directed microarray analysis showed that supplemental oxygen limited leukocyte accumulation to the infarct site by attenuation of stroke-inducible proinflammatory chemokine response. The findings provide key information relevant to understanding oxygen-dependent molecular mechanisms in the AIS-affected brain.
Journal of Cerebral Blood Flow & Metabolism (2010) **30,** 1275–1287; doi:10.1038/jcbfm.2010.7; published online 10 February 2010

Keywords: hypoxia; inflammation; ischemia; oxygen; stroke

Introduction

The human brain uses ~20% of all the oxygen consumed by the body, but represents less than 2% of total body weight (Drubach, 2000). In terms of consumption, the brain's demand for oxygen is among the highest of all organs, underscoring the importance of characterizing oxygen-sensitive mechanisms in the pathology of acute ischemic stroke (AIS) (Nemoto and Betterman, 2007). During focal ischemia, as noted during AIS, the affected tissue locus is deprived of several blood-borne supplies, including oxygen. The specific significance of AIS-caused hypoxia in the injury of the affected tissue remains obscure. Supplemental oxygen therapy, either normobaric (NBO, 100% O_2 at atmospheric pressure) or hyperbaric (HBO, 100% O_2 greater than atmospheric pressure), has long been proposed as a commonly available treatment option for stroke patients to ameliorate AIS-induced brain tissue hypoxia. Despite the support of numerous case reports (Kapp, 1979; Kapp, 1981; Price *et al*, 2004) and small-animal research (Badr *et al*, 2001; Veltkamp *et al*, 2005; Weinstein *et al*, 1987), the three clinical pilot studies that probed the efficacy of HBO to treat AIS reported little beneficial effect and cautioned about potentially harmful outcomes (Anderson *et al*, 1991; Nighoghossian *et al*, 1995; Rusyniak *et al*, 2003). Critics of the clinical pilot trials cited ill-defined treatment conditions and lack of control for thrombolytic therapy (Jain, 2003) as major limitations. Further confounding clinical trial outcome was lack of consideration or exclusion criteria for spontaneous reperfusion, which is reported to occur in 53% of cortical stroke patients within 7 days (Rha and Saver, 2007). As reperfusion injury and accompanying oxidative stress are hallmarks of stroke pathology and neuroinflammation

Correspondence: Dr S Khanna, Department of Surgery and Department of Internal Medicine, The Ohio State University Medical Center, 473 W., 12th Avenue, Columbus, OH 43210, USA. E-mail: savita.khanna@osumc.edu
This work was supported by Developmental Research Funds for stroke research from Sechrist Industries (CA) and National Healing Corporation (FL). Support was also obtained in part through NIH NS42617.
Received 1 July 2009; revised 10 December 2009; accepted 5 January 2010; published online 10 February 2010

(Wong and Crack, 2008), post-reperfusion tissue oxygenation likely has a critical role in AIS outcomes.

An overwhelmingly supportive body of preclinical research has investigated varying doses and treatment regimens for NBO and HBO in both transient and permanent models of focal stroke (Singhal, 2007). A more limited number of animal studies have directly investigated the therapeutic windows of opportunity for using supplemental oxygen in transient AIS (Badr *et al*, 2001; Lou *et al*, 2004; Veltkamp *et al*, 2005; Weinstein *et al*, 1987; Yin and Zhang, 2005). Of these, two groups have reported disparate conditions under which HBO produced both protective and harmful outcomes after reperfusion (Badr *et al*, 2001; Lou *et al*, 2004). The significance of correcting AIS-associated tissue hypoxia thus remains clouded by conflicting results.

This study was designed to specifically investigate the significance of AIS-associated focal brain hypoxia in tissue injury outcomes. Supplemental oxygen therapies were used to correct AIS-induced focal tissue hypoxia in the brain, whereas all other blood-borne supplies to the AIS-affected site remained withheld. The specific objectives were two-fold: (1) to characterize the therapeutic opportunity for using supplemental oxygen (both NBO and HBO) in two distinct and critical phases of AIS pathology, during ischemia and immediately after reperfusion, and (2) to employ high-density transcriptome screening toward generating novel hypotheses to explain how oxygen-sensitive molecular mechanisms influence the biology of AIS.

Materials and methods

Rodent Model of AIS and Reperfusion

All experiments were approved by the Institutional Animal Care and Use Committee of the Ohio State University. AIS was induced by the intraluminal suture method of MCAO as previously described, with few modifications (Khanna *et al*, 2005). Briefly, transient focal cerebral ischemia was induced in 8- to 10-week-old rats (Wistar, Harlan, Indianapolis, IN, USA) and mice (C57BL6/J; Jackson Laboratories, Bar Harbor, Maine). The rodents were anesthetized with 1 to 1.5% isoflurane delivered by medical air (21% O_2, balance N_2). A monofilament nylon suture (4-0 rat, 6-0 mouse) was advanced into the internal carotid artery by way of the external carotid artery. The filament tip was directed until slight resistance was felt ($\sim$17 mm, rat; $\sim$8 mm, mouse). Cortical blood flow was continuously monitored during surgery using laser Doppler flowmetry (LDF). Successful MCAO was confirmed by a $>$70% reduction in relative blood flow in the MCA supplied cortex. Once MCAO was verified, the rodents were brought out of anesthesia and remained conscious for 90 mins of occlusion. After 90 mins, the animals were re-anesthetized and the occluder was removed to reperfuse the MCA territory. Reperfusion was validated by LDF.

Correction of AIS-Induced Brain Hypoxia

Wistar rats were randomized into treatment groups before experimental AIS. After confirmation of successful MCAO by LDF, the rats were subjected to one of four treatment groups ($n \geqslant 5$): room air (RA), 90-min normobaric oxygen during MCAO (100% oxygen at 1ATA, iNBO), 90-min hyperbaric oxygen during MCAO (100% oxygen at 2ATA, iHBO), 90-min normobaric oxygen at reperfusion (100% oxygen at 1ATA, rNBO), and 90-min hyperbaric oxygen at reperfusion (100% oxygen at 2ATA, rHBO). Regardless of the treatment mode, all rats were housed in the same experimental hyperbaric chamber under the aforementioned conditions. The temperature inside the chamber was maintained at 25°C using a heat lamp. Mice ($n = 12$) were used for EPR oxymetry experiments and subjected to the RA, iNBO, or iHBO conditions identical to those used for rats.

Sensorimotor Assessment

To determine the effects of supplemental oxygen treatment on sensorimotor deficit after AIS, gait disturbance testing was performed on rats immediately before 48-h MRI as previously described (Bederson *et al*, 1986; Reglodi *et al*, 2003). All sensorimotor testing was performed during the light cycle, with environmental conditions consistently maintained across examinations. Briefly, an examiner masked to the experimental treatment group observed the rodent's walking pattern during a 1-minute period. A sensorimotor score on a scale of 0 to 5 was assigned to rats on the basis of their gait behavior; higher the score, greater the stroke-induced sensorimotor deficit. Straight walking, 0; walking toward the contralateral side, 1; alternate circling and walking straight, 2; alternate circling and walking toward the paretic side, 3; circling and/or other gait disturbance (backing, crawling, walking on digits), 4; and constant circling toward the paretic side, 5.

MR-Based Model Validation and Infarct Volume Determination

Magnetic resonance angiography was used to validate our MCAO model in Wistar rats and to optimize the occluder size and the internal carotid artery insertion distance for effective MCAO (Supplementary Figure S1). T2-weighted MRI was performed on anesthetized rats 48 h after MCA–reperfusion (inhalation, 1 to 1.5% isoflurane delivered by medical air) using 4.7 T MRI (Bruker Corporation, Bruker BioSpin Corporation, Billerica, MA, USA). MR images were acquired using a Rapid Acquisition with Relaxation Enhancement (RARE) sequence using the following parameters: field of view (FOV) 35×35 mm, acquisition matrix 256×256, TR 6,000 ms, TE 10.53 ms, slice gap 1.8 mm, rare factor 16, number of averages 4. Raw MR images were converted to the standard DICOM format and processed. After appropriate software contrast enhancement of images using Osirix v3.4, digital planimetry was performed by a masked observer to delineate the infarct area in each coronal brain slice. Infarct areas from brain slices were

summed, multiplied by slice thickness, and corrected for edema-induced swelling as previously described (Loubinoux *et al*, 1997), to determine infarct volume. To validate and standardize our method of infarct volume determination, we compared 48-h acquired T2-weighted images and subsequent infarct volume calculations to histological determinations of infarct volume using 2,3,5-triphenyltetrazolium viability staining (Supplementary Figure S1B–D).

EPR Oxymetry

C57BL6/J mice were selected for oxymetric studies due to a closer achievable distance between the probe and the coil as compared with that in Wistar rats, which markedly improved the signal-to-noise ratio (data not shown). Brain pO_2 measurement was performed using an *in vivo* EPR spectrometer (Magnettech, Berlin, Germany) using LiNc-BuO microcrystals for the oxymetry probe. The instrument settings were as follows: microwave frequency, 1.2 GHz (L-band); incident microwave power, 4 mW; modulation amplitude, 180 mG; modulation frequency, 100 kHz; and receiver time constant, 0.2 secs. Anesthetized mice (inhalation, 1 to 1.5% isoflurane, medical air) were stereotactically implanted with probe in the primary somatosensory cortex (S1) of the anticipated stroke-affected hemisphere (−0.1 mm bregma, +2.0 mm lateral, −1.0 mm dorsal) 1 week before MCAO. Cortical pO_2 was measured at baseline (pre-MCAO) and during ischemia under RA, iNBO, and iHBO conditions ($n \geqslant 3$). Oxymetry during ischemia was acquired within 30 mins of MCAO onset and initiation of the prescribed oxygen protocol.

Histochemical Markers of Oxidative Stress and Neurodegeneration

After MRI at 48 h, rat brain tissue was coronally sliced using a brain matrix (Ted Pella, Inc. Redding, CA, USA), formalin-fixed and embedded in paraffin. The slices were co-registered with the Paxinos' rat brain atlas (Paxinos and Watson, 2005). Coronal sections (+0.5 mm from bregma, 6 μm thick) were deparaffinized and stained in the contralateral control or ipsilateral stroke-hemispheres with anti-4-hydroxynonenal (4HNE; Cosmo Bio Ltd, Carlsbad, CA, USA), Fluoro-Jade-C (FJ; Millipore, Billerica, MA, USA), anti-8-hydroxy-2′-deoxyguanosine (8OHdG; Cosmo Bio Ltd), and anti-nitrotyrosine (NT; Sigma, St Louis, MO, USA). Quantification of positive staining was performed using the AutoMeasure module within Axiovision software (v4.6; Zeiss, Carl Zeiss Microimaging, Inc., Thornwood, NY, USA) considering representative fields of interest in the primary somatosensory (S1) cortex across groups ($n = 4$). To reduce human bias, the AutoMeasure module parameters were first standardized in the stroke-affected S1 cortex of RA animals and then applied to the remaining treatment groups.

Immunohistochemical Detection of Leukocytes

Frozen coronal brain slices (+0.5 mm from bregma) collected 48 h after MCAO reperfusion were cut into 10-μm-thick sections and mounted on slides. The sections were quick-fixed in cold acetone and immunostained with anti-myeloperoxidase (MPO; Hycult Biotech, Cell Science, Canton, MA, USA) for detection of MPO^+ leukocytes in the stroke-affected brain tissue as previously described (Breckwoldt *et al*, 2008). The AutoMeasure module within Axiovision software (v4.6, Zeiss) was used for automated quantification of MPO immunostaining. Briefly, MPO^+ leukocytes were quantified by counting the number of immunoreactive cells in four predetermined regions of the S1 somatosensory cortex of the contralateral control and stroke-affected brain tissue in RA and iHBO rats ($n \geqslant 5$).

GeneChip™ Expression Profiling

Total RNA was isolated from the infarct-affected tissue in the cerebral cortex of rats in the RA and iHBO groups. The isolated RNA was purified using the RNeasy kit (Qiagen, Valencia, CA, USA) and quality was checked using an Experion Electrophoresis System (Bio-Rad, Hercules, CA, USA). The targets for microarray hybridization were prepared as previously described (Roy *et al*, 2006). Briefly, samples were hybridized for 16 h at 45°C to GeneChip Test-2 arrays to assess the preparation quality (Affymetrix, Santa Clara, CA, USA). On verification of sample quality, the targets were hybridized to Affymetrix rat genome arrays (rat genome 230 v2.0) in the same manner as the Test-2 arrays. The arrays were washed, stained with streptavidin–phycoerythrin, and scanned with a GeneArray scanner. Raw data from the GeneChip Operating Software (GCOS, version 1.0) was imported for analysis using Stratagene ArrayAssist (version 4.0). Background adjustment and quantile normalization of data were performed using the GeneChip Robust Multi-Array Average (GCRMA) summarization. To determine differential gene expression candidates between RA and iHBO, significance analysis testing was performed using Student's two-class *t*-test ($P < 0.05$), Benjamini–Hochberg false discovery rate correction, and a fold change cut-off value >2.0. Clusters of genes differentially expressed in the RA and iHBO groups were functionally categorized using DAVID (Database for Annotation, Visualization and Integrated Discovery; NIAID, NIH). See Figure 4 for the GeneChip workflow schema.

Laser Microdissection Pressure Catapulting

Brain tissue was cut into 2-mm coronal sections in a matrix after which it was embedded and frozen in OCT compound (Sakura, Torrance, CA, USA). The embedded brains were sliced into 12-μm-thick sections using a cryostat (CM3050s; Leica, Leica Microsystems Inc., Bannockburn, IL, USA) and mounted on RNAZap-treated thermoplastic (polyethylene napthalate)-covered glass slides (PALM Technologies, Bernreid, Germany). The slides were incubated in RNA-later RNA stabilization reagent (Applied Biosystems/Ambion, Austin, TX, USA) for 4 mins. To collect neurons from the control and stroke S1 cortex, neurons were rapidly immunostained with anti-NeuN antibody (Millipore, Billerica, MA, USA) and selectively captured as previously described (Roy *et al*, 2007). For detection of

leukocyte p47phox gene expression, 800,000-μm^2 regions of control and stroke-affected S1 cortex were collected from the same brain section. All elements were captured using a PALM MicroLaser, MicroBeam, and RoboStage/RoboMover system for high-throughput sample collection. After laser cutting, the elements were catapulted directly into 30 µl of RNA extraction buffer (PicoPure RNA Isolation kit; Arcturus, Mountain View, CA, USA) situated directly above the section in a microtube cap. After RNA isolation, RNA quality was checked using Experion Electrophoresis System Hi-Sense chips (Bio-Rad, Hercules, CA, USA) as described previously (Roy *et al*, 2007).

Real-Time PCR Validation of Candidate Genes

The expression levels of candidate genes were independently determined at 12- and 48-h time points using real-time PCR. Briefly, total RNA (250 ng) was reverse-transcribed into cDNA using an oligo-dT primer and Superscript II. Reverse transcription-generated DNA was quantified by real-time PCR assay using the double-stranded DNA-binding dye SYBR Green-I. Relative gene expression was standardized to 18s rRNA. Data are shown as means ± s.d. Primer sequences provided in Supplementary Figure S2.

Statistical Considerations

Statistical analysis of data was performed using SPSS Statistics software (v17.0). All data are reported as mean ± s.d. Difference between means was tested using Student's *t*-test or one-way ANOVA with Tukey's *post hoc* test where appropriate ($P < 0.05$).

Results

The Limited Temporal Window of Opportunity for Supplemental Oxygen Therapy in AIS

Successful MCAO was validated across treatment groups by a reduction in MCA-supplied cortical blood flow of >70%. After induction of MCAO, rats were immediately removed from anesthesia and brought to the experimental chamber where they were subjected to RA, iNBO, iHBO, rNBO, or rHBO experimental conditions (Figure 1A). Subsequent to 90 mins of ischemia, the MCA area was reperfused by withdrawing the occluder from the origin of the MCA and rats were returned to the experimental chamber to continue their prescribed oxygen regimen. No significant difference was observed across the treatment groups using LDF-measured cortical blood flow upon induction of MCAO or immediately after reperfusion (Figure 1B).

Strikingly, iNBO and iHBO treatment significantly reduced AIS infarct volume at 48 h as compared with RA controls by more than 50% (Figures 1C and 1D). Although there was a trend for smaller lesion volumes in iHBO as compared with iNBO animals, the difference was not statistically significant. In contrast to the observed attenuation of infarct volume by supplemental oxygen during ischemia, rNBO and rHBO significantly exacerbated the AIS-induced lesion volume: in the case of rHBO by greater than 30% over RA and greater than 70% when compared with iNBO and iHBO treatments. Of note, the observed MRI outcomes closely matched the 2,3,5-triphenyltetrazolium viability staining of brain tissue (Supplementary Figure S1). Colorless 2,3,5-triphenyltetrazolium is enzymatically reduced to a red formazan product by dehydrogenases abundant in the mitochondria and stain intensity correlates with the number and functional activity of mitochondria in brain tissue (Benedek *et al*, 2006; Goldlust *et al*, 1996).

Gait disturbance testing of post-stroke sensorimotor function showed that iNBO and iHBO treatment significantly improved post-stroke locomotion as compared with RA controls. While rNBO and rHBO sensorimotor function was not statistically worse than that in the RA controls, gait deficit was significantly worse when compared with that in iNBO- and iHBO-treated rats (Figure 1E). Thus, we noted specific conditions under which supplemental oxygen therapy may be helpful or harmful. These observations led us to examine the impact of supplemental oxygen therapy and timing of delivery on oxidative stress and neurodegeneration associated with AIS.

Elevated levels of lipid peroxidation (4HNE), protein (NT), and nucleic acid (8OHdG) oxidation were observed at 48 h after reperfusion in the S1 cortex of the stroke-affected hemisphere in RA rats as compared with contralateral control tissue (Figure 2). In iNBO- and iHBO-treated animals, markers of oxidative stress were less prominent in the matching S1 cortical region. In concordance with AIS-induced lesion volume data, rHBO induced overt oxidative stress at the stroke site when compared to RA, iNBO and iHBO animals. Noteworthy, rHBO animals also showed gross morphological differences in the AIS-affected sections in the form of tissue fragmentation and pyknosis. rNBO animals did not show elevated levels of oxidative stress markers or neurodegeneration as compared with RA controls.

FJ stains degenerating neurons (Schmued and Hopkins, 2000). Prominent neurodegeneration was observed in cortical tissue from rats subjected to rHBO as compared with RA controls (Figure 2). iHBO rodents showed attenuated neurodegeneration as compared with both RA and rHBO animals. No statistically significant difference in neurodegeneration was observed between the rNBO and RA groups.

In light of the observation that supplemental oxygen therapy attenuates AIS-mediated damage during occlusion, but not after reperfusion, we sought to elucidate the molecular mechanisms of oxygen-mediated protection. The approach adopted included EPR oxymetry to determine the efficacy of supplemental oxygen therapy during ischemia to

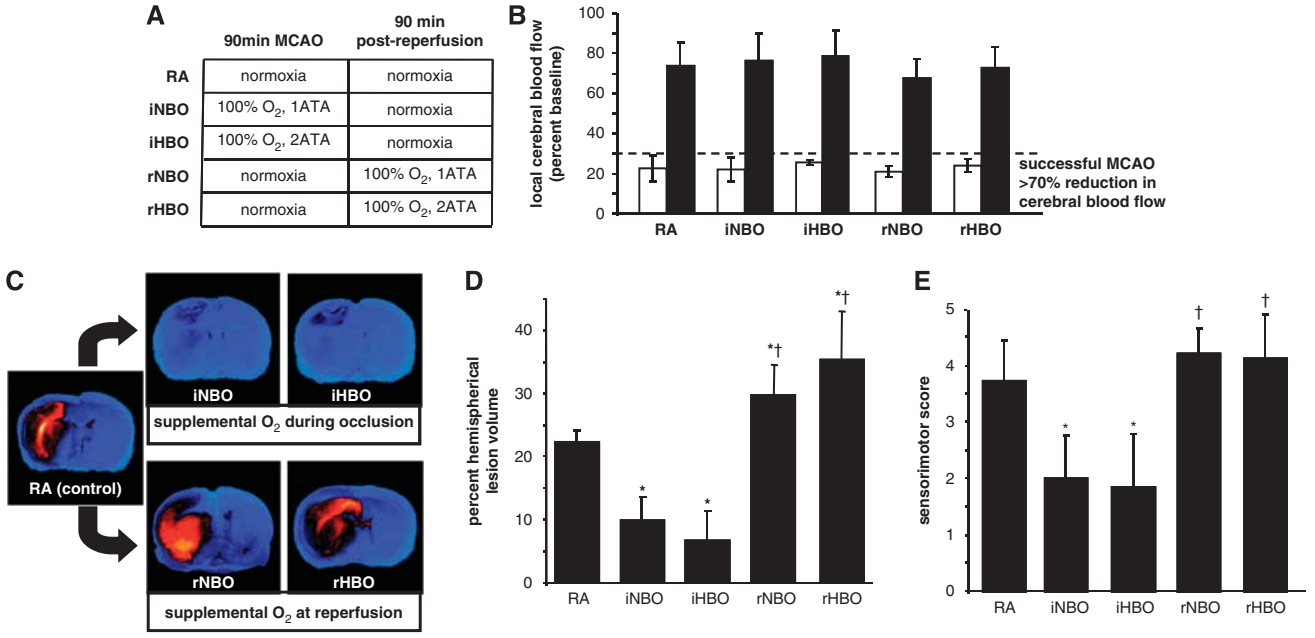

Figure 1 Supplemental oxygen therapy reduces during, exacerbates at reperfusion, the AIS infarct volume. (**A**) Oxygen therapy treatment groups. (**B**) Mean local cerebral blood flow across treatment groups from the stroke-affected MCA area (−0.1 mm bregma, + 2.0 mm lateral) at the onset of ischemia (white bar) and upon reperfusion (black bar) relative to baseline. Successful MCAO was validated by a > 70% reduction in the MCA-area blood flow. (**C**) T2-weighted MRI taken 48 h after MCAO under RA, iNBO, iHBO, rNBO, and rHBO conditions. Color look up table applied—shift from blue to red denotes edema and stroke-induced infarct. One representative image from each group. (**D**) Percent hemispherical infarct volume corrected for edema calculated from T2-weighted MR images ($n \geqslant 5$). (**E**) Gait disturbance testing performed 48 h after MCA reperfusion to assess sensorimotor function. $^{*}P < 0.05$ versus RA; $^{\dagger}P < 0.05$ versus iNBO, iHBO.

correct stroke-affected brain pO_2 and subsequent unbiased query of the brain transcriptome with the objective to profile oxygen-sensitive genes in the AIS-affected brain. Results from such approach would help generate novel hypotheses aimed at explaining how correction of AIS-associated focal hypoxia of the brain may influence injury outcomes. In this study 'oxygen-sensitive' refers to primary and secondary biological outcomes that were sensitive to supplemental oxygen therapy.

Supplemental Oxygen Corrects AIS-Induced Hypoxia

To determine the effects of MCAO-induced hypoxia on stroke-affected tissue pO_2, we used particulate-based EPR oxymetry in mice. The benefits of EPR oxymetry over probe-based approaches include improved accuracy, resistance to drifting, repeatability, and non-invasive measurement at the time of signal acquisition (Vikram *et al*, 2007). EPR probes were selectively implanted in the salvageable penumbral tissue of the stroke-affected S1 cortex observed to be protected in animals subjected to iNBO and iHBO as compared with those treated with RA (Figure 3A). Representative EPR spectra from baseline, RA, iNBO, and iHBO animals show the difference in peak-to-peak width in response to tissue pO_2 (Figure 3B). MCAO-induced ischemia under RA stroke conditions resulted in a 50% reduction in stroke-affected tissue pO_2 as compared with baseline (pre-stroke) levels. iNBO therapy restored penumbral tissue pO_2 during the occlusion event, improving tissue oxygenation above the RA stroke and baseline conditions (Figure 3C). Importantly, this work demonstrates non-contact EPR oxymetry of the stroke affected brain *in vivo* under iHBO conditions for the first time. Although iHBO improved the pO_2 in stroke-affected penumbra above baseline and ischemia values as did iNBO, the observed effect on tissue pO_2 was no greater than that using iNBO treatment.

The Oxygen-Sensitive Transcriptome in AIS-Affected Brain

On the basis of EPR evidence supporting the ability of iHBO to correct brain tissue pO_2 during MCAO and the significant attenuation of AIS-induced neurodegeneration observed by FJ staining, we sought to use iHBO to identify the oxygen-sensitive transcriptome during AIS. GeneChip data mining was directed at elucidating oxygen-sensitive genes within the stroke-affected brain tissue that were differentially regulated in the presence or absence of iHBO. Figure 4A illustrates the adapted data analysis

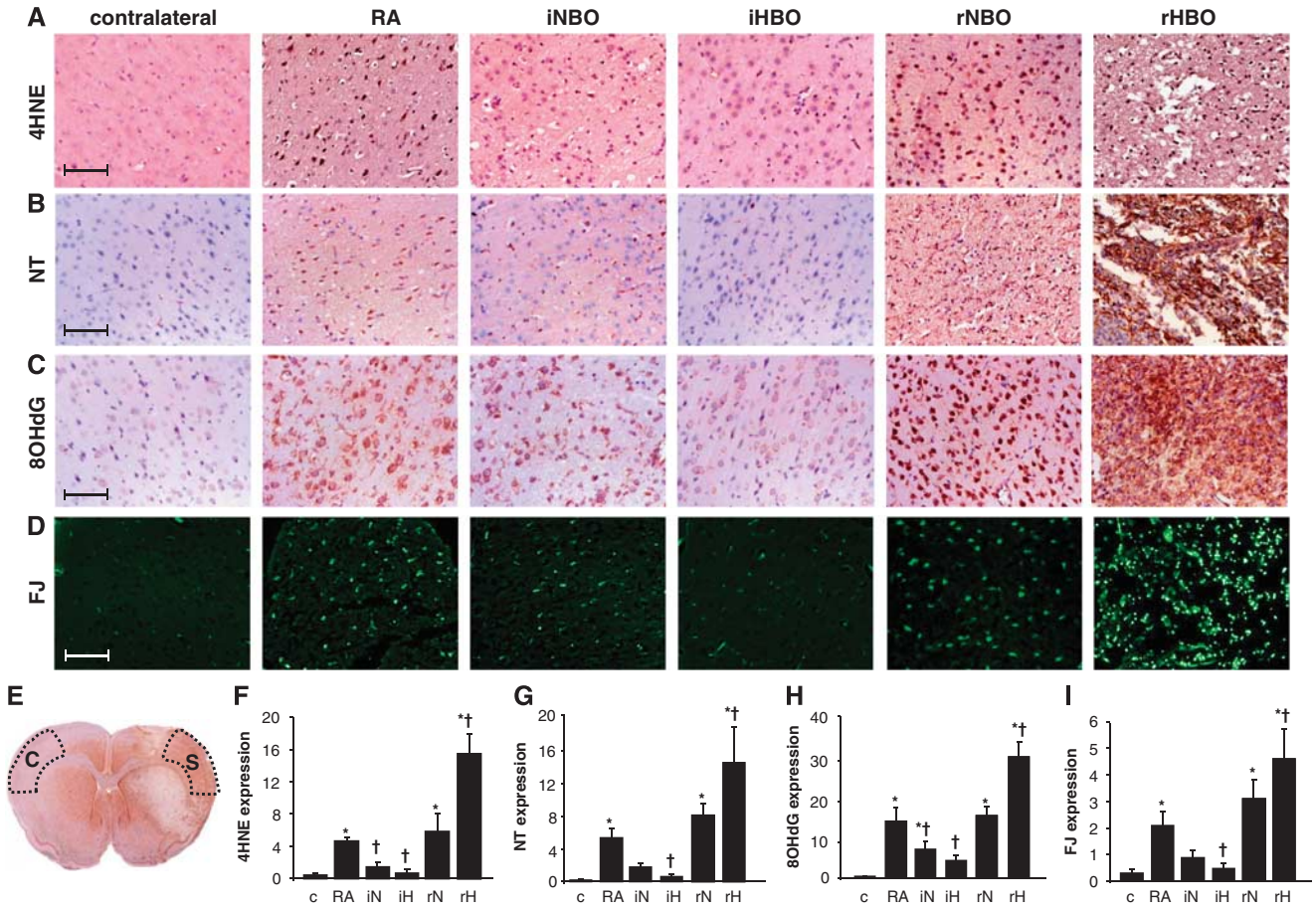

Figure 2 Oxidative stress and neurodegeneration after supplemental oxygen therapy in AIS. Representative $\times 20$ FOV images of lipid peroxidation (**A**, 4HNE), protein oxidation (**B**, NT), nucleic acid oxidation (**C**, 8OHdG), and neuron-specific degeneration marker FJ (**D**) in the contralateral and stroke-affected (RA, iNBO, iHBO, rNBO, rHBO) S1 cortex 48 h after MCAO. Bar = 100 μm. (**E**) A representative coronal section showing the contralateral (c) and stroke (s) hemisphere S1 cortex after 4HNE staining from which $\times 20$ FOV images were captured. (**F–I**) Quantification of expression (% area) was determined from the S1 cortex ($n \geqslant 5$) for 4HNE, NT, 8OHdG, and FJ. $^{*}P < 0.05$ versus c; $^{\dagger}P < 0.05$ versus RA. Bar = 100 μm.

scheme, which is based on previous work by our group (Roy *et al*, 2006). Of the 31,099 probesets analyzed, 3,281 were upregulated and 2,488 were downregulated in response to HBO therapy during AIS. The heat map generated from the analyzed microarray data illustrates the tight consistency in gene expression within and across the experimental groups (Figure 4B). The volcano plot visually shows the expression pattern of the differentially expressed probe sets between the groups (Figure 4C). Functional categorization of differentially expressed genes with a greater than twofold change was performed using DAVID and visualized in KEGG pathways.

Table 1 contains an abridged list of key oxygen-sensitive genes and functional pathways in AIS identified through data analysis. The represented functional categories were selected on the basis of annotation clusters with the highest Expression Analysis Systematic Explorer (EASE) scores, calculated from a modified Fisher exact test for identification of biological themes from microarray data (Hosack *et al*, 2003). Verification of microarray results was performed using laser microdissection pressure catapulting for cell-type and region-specific analyses. The relative gene expression of the cortical neuron subtype markers was not significantly different across laser capture microdissection collected treatment groups (Supplementary Figure S2A). Neither was there a significant difference in gene expression in the sham-operated animals kept under normoxia (RA) or subjected to 90 mins of HBO (100% O_2 at 2ATA) (Supplementary Figure S2B). AIS-affected and contralateral control neurons from the S1 cortex were quick-stained with anti-NeuN antibody and then laser-microdissected and captured for GeneChip validation (Figures 5A and 5B). Real-time PCR quantification of neurofilament-L and glial fibrillary acidic protein (GFAP) expression show the neuron specificity of the captured elements (Figure 5C). The selected gene candidates for real-time PCR validation were chosen from the repre-

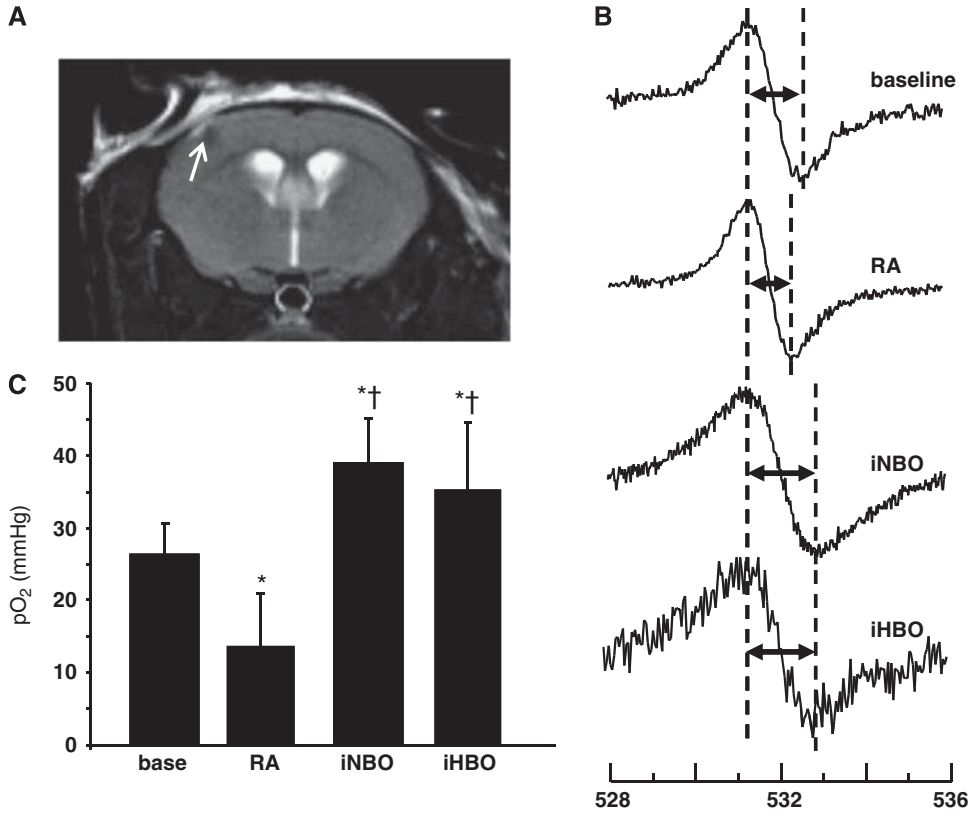

Figure 3 Supplemental oxygen therapy corrects penumbral tissue pO_2 during MCAO. (**A**) A LiNc-BuO probe was stereotactically implanted into the S1 cortex using the following coordinates: −0.1 mm bregma, +2.0 mm lateral, −1.0 mm dorsal. Probe placement was assessed using MRI (arrow). (**B**) One week after probe delivery, EPR spectra were acquired and averaged from 60-s scans ($n = 10$) at baseline (before MCAO) and during MCAO in animals subjected to RA, iNBO, and iHBO conditions ($n \geqslant 3$). (**C**) The peak-to-peak width of the EPR spectra was used to calculate pO_2 using a standard calibration curve. $^*P < 0.05$, baseline versus RA; $^\dagger P < 0.05$, RA versus iNBO.

sented DAVID functional pathways with >2-fold change in expression. The downregulated gene candidates (iHBO versus RA) included monocyte-chemoattractant protein-1 (MCP1) and interleukin-6 (Figures 5D and 5E). Upregulated genes included neural cell adhesion molecule and glutamate oxaloacetate transaminase-1 (Figures 5F and 5G). The findings of quantitative real-time PCR assays validated the adopted DNA microarray analysis and data mining approach.

Supplemental Oxygen during AIS Inhibits Proinflammatory Leukocyte Recruitment

Taken together, the differential regulation of gene targets associated with proinflammatory cytokines (Table 1, indicated in bold) and the observed differences in the markers of oxidative stress across treatment groups suggested that supplemental oxygen during AIS modulated post-reperfusion inflammation. These important clues led us to investigate the presence of proinflammatory leukocytes in the stroke-affected cortex under RA and iHBO conditions. MPO protein is commonly used to identify leukocytes (including neutrophils, macrophages, and monocytes) in stroke-affected tissue (Breckwoldt *et al*, 2008; Lee *et al*, 2008; Yamagami *et al*, 1999). MPO interacts with hydrogen peroxide to generate highly reactive species, including hypochlorite (OCl−) (Breckwoldt *et al*, 2008). MPO-mediated radicalization of molecules induces apoptosis and nitrotyrosination of proteins and has been shown to have a major role in animal models of stroke in mediating the post-ischemic inflammatory response (Lau and Baldus, 2006; Matsuo *et al*, 1994; Takizawa *et al*, 2002). Significantly fewer MPO^+ leukocytes and decreased intensity of MPO^+ immunostaining were observed in the stroke-affected S1 cortex of RA- and iHBO-treated rats 48 h after reperfusion (Figures 6A–6C).

In addition to MPO, leukocytes generate potent oxygen free radical species, including superoxide (O_2^-), through the NADPH oxidase complex (Chen *et al*, 2009). NADPH oxidase-mediated generation of O_2^- is known to contribute to reperfusion injury after AIS through oxidative damage to lipids, proteins, and nucleic acids (Chan, 2001). Leukocyte NADPH

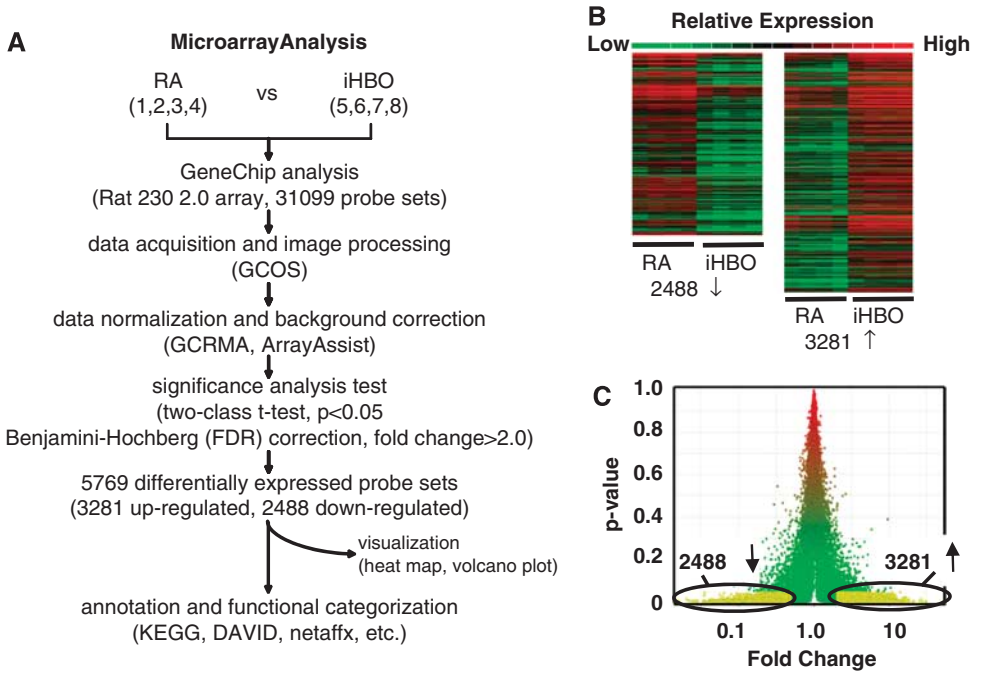

Figure 4 Microarray analysis of the oxygen-sensitive transcriptome in AIS. (**A**) A flow chart depicting the microarray analysis process. After normalization and Benjamini–Hochberg false discovery correction, 5,769 differentially expressed probesets were identified assuming a twofold or greater increase/decrease in expression and a significance value of $P < 0.05$. (**B**) Heat-map visualization of differentially expressed probes—2,488 probes with lower expression and 3,281 probes with higher expression in iHBO-treated stroke tissue as compared with that in RA-treated tissue. (**C**) A volcano plot depicting the rodent transcriptome, with the oxygen-sensitive subset highlighted in yellow.

Table 1 An abridged list of oxygen-sensitive genes up- and downregulated in response to iHBO therapy

Functional pathway	*Gene name*	*Fold change (iHBO versus RA)*	*Regulation*
Proinflammatory cytokines	**Monocyte-chemoattractant protein-1**	**6.25**	**Down**
	Interleukin-6	**4.25**	**Down**
	Intercellular adhesion molecule-1	**5.34**	**Down**
Apoptosis	Caspase-1, 6, 8	3.29, 2.23, 2.37	Down
	Matrix metalloproteinase-12	8.63	Down
	p53	2.25	Down
	TNF-α	6.63	Down
Complement/coagulation	Cyclin-D	2.77	Down
	Thrombomodulin	5.83	Down
	Von Willebrand factor	5.43	Down
BBB integrity	Cadherin-10	2.09	Up
	Claudin-10, 11	4.06, 2.01	Up
	MAGI1	2.55	Up
	Tubulin, α4a	2.27	Up
K^+ channels	Kir 4, 6, 11	3.97, 4.41, 4.89	Up
	Kv1, 2, 4	2.77, 5.40, 3.47	Up
Glutamate metabolism	Glutamate decarboxylase-1	4.06	Up
	Glutamate oxaloacetate transaminase-1	3.54	Up
	Glutaminase	3.36	Up
Axon guidance	Neural cell adhesion molecule-1	2.88	Up
	Plexin-B	3.25	Up
	Roundabout axon guidance receptor	2.24	Up

Abbreviations: BBB, blood–brain barrier; iHBO, hyperbaric oxygen during ischemia; RA, room air; TNF, tumor necrosis factor.
Fold change is calculated as the absolute ratio of normalized intensities between the average intensities of the grouped samples.

oxidase subunit p47phox gene expression was significantly lower in the LCM-captured penumbra tissue from the iHBO S1 cortex as compared with that in RA animals (Figure 6D).

Discussion

Differences in AIS outcomes associated with iNBO/iHBO and rNBO/rHBO provide evidence of benefit

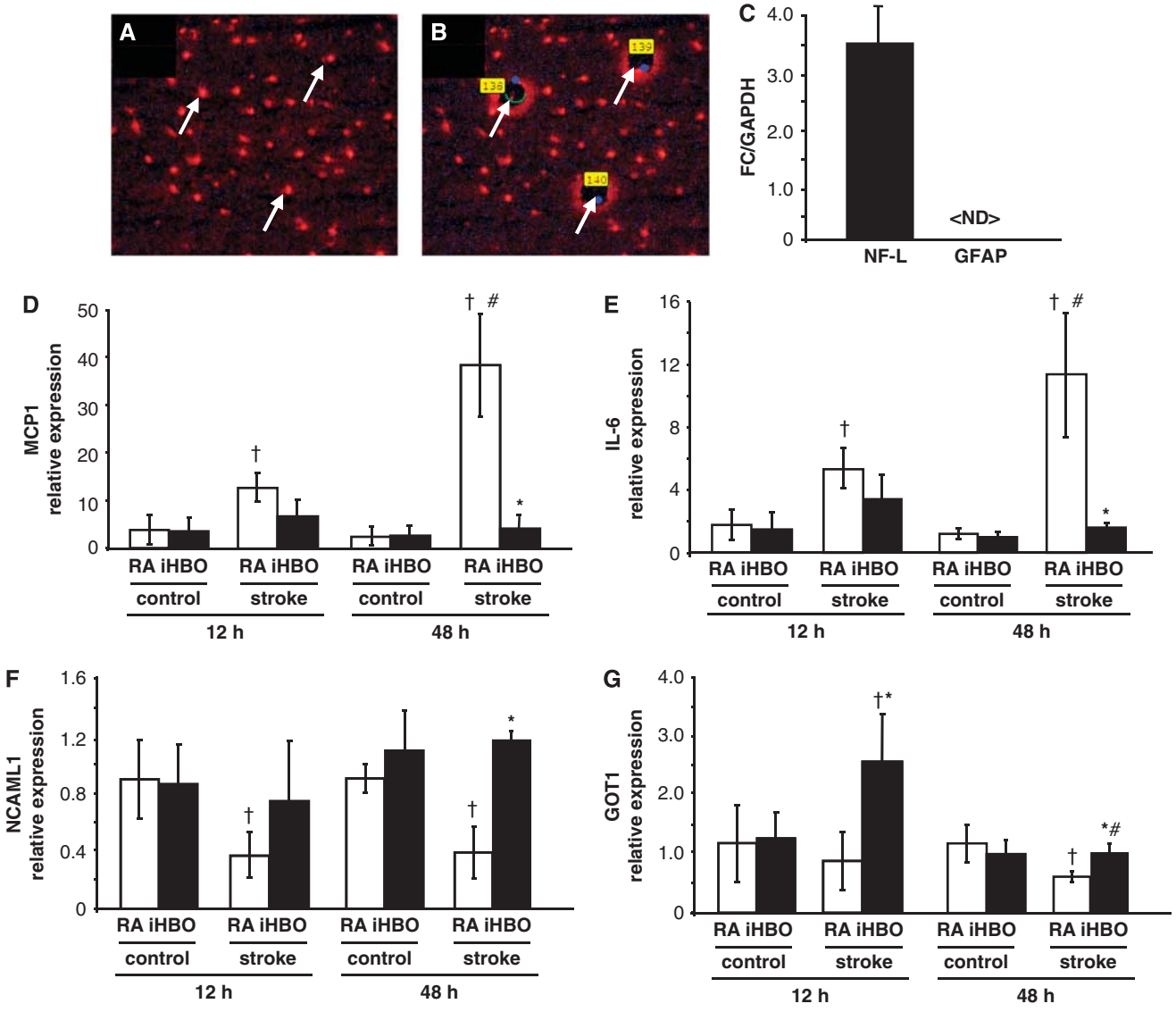

Figure 5 Laser microdissection pressure catapulting and real-time quantitative–PCR validation of microarray targets. (**A** and **B**) Neurons of S1 cortex were rapidly stained for anti-NeuN and captured (arrows) by laser microdissection pressure catapulting. (**C**) To verify the specificity of the captured elements, gene expression of a neuronal (NF-L) and a glial marker (GFAP) was checked by real-time PCR. (**D**–**G**) Expression of oxygen-sensitive candidate genes was validated by real-time PCR in the stroke-affected (ischemic) and contralateral (control) neurons from RA and iHBO animals at 12- and 24-h time points. (**D**) MCP1, (**E**) interleukin-6, (**F**) neural cell adhesion molecule-L1, and (**G**) glutamate oxaloacetate transaminase. < ND >, not detectable. $^{*}P < 0.05$, RA stroke versus iHBO stroke at a given time point; $^{\dagger}P < 0.05$, control versus stroke within the oxygen therapy group at a given time point; $^{\#}P < 0.05$, same group, the 12- versus the 48-h time point.

for supplemental oxygen therapy with significant protection during the AIS event, but deleterious consequences at reperfusion. While there are previous reports of beneficial and detrimental outcomes associated with post-reperfusion HBO ($\geqslant$3 h after reperfusion), this study characterizes a 90-min period of time at the onset of reperfusion in which AIS-affected tissue is susceptible to oxygen-mediated exacerbation of stroke lesion volume.

Badr *et al* (2001) documented the beneficial outcomes for HBO (3ATA, 60 mins) in rats subjected to transient MCAO at 3 and 6 h after reperfusion, but not at 12 and 23 h. Lou *et al* (2004) reported similar results using the same HBO dose and duration at 3, 6, and 12 h after reperfusion. On the basis of the outcomes from these time points, both groups concluded that the therapeutic window of opportunity for HBO in AIS should be restricted to <6 h after reperfusion. The results from this study, however, point to an acute phase of reperfusion (<90 mins after reperfusion) for which supplemental oxygen therapy is contraindicated. Indeed, mediators of oxidative stress, such as superoxide anion (O_2^-), are increased in AIS-affected brain tissue within 1 h after

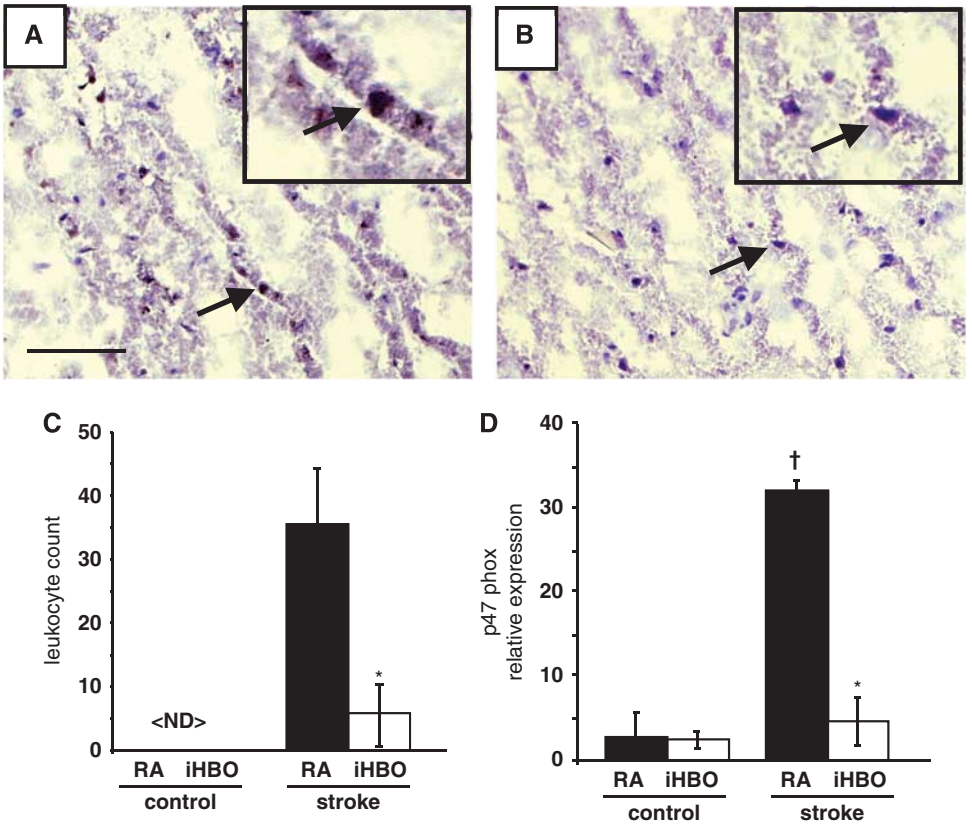

Figure 6 Supplemental oxygen during AIS attenuates proinflammatory leukocyte accumulation in stroke-affected tissue. Representative $\times 20$ FOVs from the stroke-affected S1 cortex show increased intensity and number of MPO^+ leukocytes (brown) in RA-treated animals (**A**) as compared with that in iHBO-treated animals (**B**). The black arrow indicates leukocyte at $\times 20$ selected for the enlarged view in the inset. MPO^+ leukocytes were not detected in contralateral control tissue (not shown). (**C**) Quantification of MPO^+ leukocytes from representative control and stroke FOVs of RA- and iHBO-treated animals ($n \geqslant 5$). (**D**) The relative gene expression of NADPH oxidase subunit p47phox, a key mediator of leukocyte-mediated respiratory burst, in the stroke-affected cortex laser-captured from iHBO brain tissue as compared with that in the RA control. $^*P < 0.05$, iHBO versus RA; $^\dagger P < 0.05$, RA stroke versus RA control. Bar = 100 μm.

reperfusion (Kim *et al*, 2002). Our data suggest that supplemental oxygen during reperfusion results in an oxygen-rich environment in which oxidative stress and cerebral reperfusion injury intensifies. As acute reactive oxygen species generation wanes several hours after reperfusion (Kim *et al*, 2002), NBO and HBO therapies (3 to 6 h after reperfusion) may again prove beneficial in response to secondary inflammatory mediators such as neutrophils.

Taken together our results support the concept of a dual significance for oxygen therapy in AIS, which can be either beneficial or harmful depending on the timing of application. This finding likely explains the mixed outcomes reported in small-animal and clinical stroke studies. Whereas clinical pilot studies found no benefit and potentially harmful outcomes associated with supplemental oxygen therapy, a majority of clinical case reports and small-animal studies have reported favorable results related to both post-stroke infarct volume and functional assessment (Singhal, 2007). Importantly, clinical pilots studies (Anderson *et al*, 1991; Nighoghossian *et al*, 1995; Rusyniak *et al*, 2003) associated with inconclusive or negative outcomes did not control for supplemental oxygen treatments in time windows that overlapped with thrombolytic therapy (Jain, 2003). Poor clinical pilot trial design, which lacked exclusion criteria accounting for the heterogeneity of the human stroke condition, has tempered the enthusiasm for supplemental oxygen as a viable therapeutic option in AIS. Improved diagnostic processes are needed in the clinic to identify human stroke conditions that could benefit from supplemental oxygen therapy. Non-invasive methods to rapidly and repeatedly monitor cerebrovascular perfusion in AIS patients would benefit the clinical prescription of supplemental oxygen therapy.

This work describes for the first time the use of non-contact oxymetry for the stroke-affected brain cortex during ischemia within an HBO chamber. This important distinction is in contrast to previous work in which animals received HBO treatment during ischemia but were removed from the chamber for EPR oxymetry acquisition (Hou *et al*, 2007). Here,

we show that both iNBO and iHBO therapies are effective in correcting the pO_2 of stroke-affected tissue during ischemia. Contrary to our hypothesis, however, no significant difference was observed in brain pO_2 measurements from the ischemic penumbra in animals receiving iNBO and iHBO treatment. Although unexpected, this observation was consistent with stroke outcome data. As previously noted, both iNBO and iHBO attenuated AIS-induced lesion volume and improved functional outcome (sensorimotor score). However, histological determination of neurodegeneration in the AIS-affected cortex was significantly less with iHBO treatment, not iNBO.

Tissue pO_2 represents a dynamic balance between oxygen delivery and consumption. When hemoglobin is fully saturated with oxygen, three factors contribute to brain pO_2: cerebral blood flow, partial pressure of oxygen in arterial blood, and changes in metabolic rate for oxygen (Calvert *et al*, 2007; Demchenko *et al*, 2005). HBO treatment is known to induce cerebral vasoconstriction in the rodent brain, which may buffer against oxygen toxicity at high brain-tissue pO_2 (Demchenko *et al*, 2001; Demchenko *et al*, 2005). During HBO treatment, such regulatory mechanisms are perhaps aimed at protecting the brain, rich in unsaturated fatty acid, against the risk of oxygen toxicity at high pO_2.

In this study, no significant difference in local cerebral blood flow was observed across treatment groups at the onset of ischemia (before iNBO/iHBO) or immediately after reperfusion (before rNBO/rHBO). However, LDF readings were taken to validate the success of the experimental stroke model and consequently acquired outside of supplemental oxygen treatments. Additional oxymetry time points and longer assessment of brain pO_2 during the ischemic episode under RA, iNBO, and iHBO conditions are warranted for future study.

We used supplemental oxygen treatment during ischemia (iHBO) as a tool to delineate oxygen-sensitive gene networks in AIS, whereas other etiological contributors, such as arrest of glucose transport, remained unchanged. The total number of genes that responded to supplemental oxygen treatment during AIS represented $\sim$20% of the queried rodent transcriptome. Of the gene candidates validated with real-time PCR, none were observed to be differentially expressed by HBO alone, qualifying that the selected gene candidates are oxygen-sensitive only in the context of AIS. A simplified interpretation of this observation is that supplemental oxygen during 90-min AIS affords protection by maintaining the high respiratory and energy demands obligated by the central nervous system. As such, homeostatic CNS function is preserved, accounting for no observable difference in gene expression between the control and stroke hemispheres when select gene candidates were validated using real-time PCR. Without glucose, the preferred metabolic substrate for brain, this conclusion however plausible is unlikely.

Probing deeper into the outcomes of our microarray analysis, we identified proinflammatory cytokine signaling as a highly relevant functional pathway given the striking differences in the markers of oxidative stress across treatment groups. MCP1 is classically defined as a chemokine with the ability to induce directed chemotaxis of monoctyes and basophils (Leonard and Yoshimura, 1990). Recent evidence supports MCP1-mediated recruitment of neutrophils to stroke-affected tissue as well (Dimitrijevic *et al*, 2007; Reichel *et al*, 2009). MCP1 gene expression is induced within 6 h after rodent MCAO/reperfusion and reaches its highest expression level between 24 and 48 h (Wang *et al*, 1995; Yamagami *et al*, 1999). In our study, notable induction of MCP1 gene expression was observed in the stroke-affected neurons of RA, but not iHBO, rodents. Intercellular adhesion molecule-1 has also been implicated in ischemia/reperfusion injury through chemoattraction of polymorphonuclear leukocytes, including neutrophils (Deng *et al*, 2003; Justicia *et al*, 2003). Leukocytes accumulate in the stroke-affected brain within 24 h of AIS onset (Price *et al*, 2004) and mediate inflammation through of superoxide radicals by NADPH oxidase (Lambeth, 2004). Inhibition of NADPH oxidase expression has been reported to be neuroprotective in mice subjected to MCAO (Chen *et al*, 2009).

Importantly, this work is the first to show that correction of AIS–hypoxia with iHBO treatment significantly inhibits MCP1 and intercellular adhesion molecule-1 expression during the acute inflammatory phase ($<$48 h) after MCAO reperfusion. In response, leukocyte accumulation and NADPH oxidase subunit p47phox gene expression in stroke-affected tissue were also significantly less under conditions of iHBO treatment as compared with that in the RA controls. Inhibition of proinflammatory cytokine gene expression by iHBO may therefore ease post-reperfusion reactive oxygen species-mediated inflammation by inhibiting leukocyte chemoattraction and subsequent NADPH oxidase activity at the stroke site.

In conclusion, this work delineates between two critical phases of AIS, during occlusion and immediately after reperfusion, in which supplemental oxygen produced disparate outcomes. During AIS, supplemental oxygen attenuated the AIS outcomes and markers of oxidative stress, whereas upon reperfusion supplemental oxygen exacerbated AIS injury. In light of these observations, we used supplemental oxygen during ischemia to correct the hypoxia component of AIS injury and to characterize the oxygen-sensitive molecular mechanisms of AIS pathology. Proinflammatory chemokine signaling and subsequent accumulation of leukocytes to stroke-affected tissue were attenuated with iHBO therapy. The outcomes of the microarray study point toward novel hypotheses aimed at understanding the molecular basis of the significance of tissue oxygenation in AIS.

Conflict of interest

The authors declare no conflict of interest.

References

Anderson DC, Bottini AG, Jagiella WM, Westphal B, Ford S, Rockswold GL, Loewenson RB (1991) A pilot study of hyperbaric oxygen in the treatment of human stroke. *Stroke* 22:1137–42

Badr AE, Yin W, Mychaskiw G, Zhang JH (2001) Dual effect of HBO on cerebral infarction in MCAO rats. *Am J Physiol Regul Integr Comp Physiol* 280:R766–70

Bederson JB, Pitts LH, Tsuji M, Nishimura MC, Davis RL, Bartkowski H (1986) Rat middle cerebral artery occlusion: evaluation of the model and development of a neurologic examination. *Stroke* 17:472–6

Benedek A, Moricz K, Juranyi Z, Gigler G, Levay G, Harsing Jr LG, Matyus P, Szenasi G, Albert M (2006) Use of TTC staining for the evaluation of tissue injury in the early phases of reperfusion after focal cerebral ischemia in rats. *Brain Res* 1116:159–65

Breckwoldt MO, Chen JW, Stangenberg L, Aikawa E, Rodriguez E, Qiu S, Moskowitz MA, Weissleder R (2008) Tracking the inflammatory response in stroke *in vivo* by sensing the enzyme myeloperoxidase. *Proc Natl Acad Sci USA* 105:18584–9

Calvert JW, Cahill J, Zhang JH (2007) Hyperbaric oxygen and cerebral physiology. *Neurol Res* 29:132–41

Chan PH (2001) Reactive oxygen radicals in signaling and damage in the ischemic brain. *J Cereb Blood Flow Metab* 21:2–14

Chen H, Song YS, Chan PH (2009) Inhibition of NADPH oxidase is neuroprotective after ischemia–reperfusion. *J Cereb Blood Flow Metab* 29:1262–72

Demchenko IT, Boso AE, Whorton AR, Piantadosi CA (2001) Nitric oxide production is enhanced in rat brain before oxygen-induced convulsions. *Brain Res* 917:253–61

Demchenko IT, Luchakov YI, Moskvin AN, Gutsaeva DR, Allen BW, Thalmann ED, Piantadosi CA (2005) Cerebral blood flow and brain oxygenation in rats breathing oxygen under pressure. *J Cereb Blood Flow Metab* 25:1288–300

Deng H, Han HS, Cheng D, Sun GH, Yenari MA (2003) Mild hypothermia inhibits inflammation after experimental stroke and brain inflammation. *Stroke* 34:2495–501

Dimitrijevic OB, Stamatovic SM, Keep RF, Andjelkovic AV (2007) Absence of the chemokine receptor CCR2 protects against cerebral ischemia/reperfusion injury in mice. *Stroke* 38:1345–53

Drubach D (2000) *The Brain Explained*. Upper Saddle River, NJ: Prentice Hall Health

Goldlust EJ, Paczynski RP, He YY, Hsu CY, Goldberg MP (1996) Automated measurement of infarct size with scanned images of triphenyltetrazolium chloride-stained rat brains. *Stroke* 27:1657–62

Hosack DA, Dennis Jr G, Sherman BT, Lane HC, Lempicki RA (2003) Identifying biological themes within lists of genes with EASE. *Genome Biol* 4:R70

Hou H, Grinberg O, Williams B, Grinberg S, Yu H, Alvarenga DL, Wallach H, Buckey J, Swartz HM (2007) The effect of oxygen therapy on brain damage and cerebral pO(2) in transient focal cerebral ischemia in the rat. *Physiol Meas* 28:963–76

Jain KK (2003) Hyperbaric oxygen in acute ischemic stroke. *Stroke* 34:e153; author reply e153–e155

Justicia C, Panes J, Sole S, Cervera A, Deulofeu R, Chamorro A, Planas AM (2003) Neutrophil infiltration increases matrix metalloproteinase-9 in the ischemic brain after occlusion/reperfusion of the middle cerebral artery in rats. *J Cereb Blood Flow Metab* 23:1430–40

Kapp JP (1979) Hyperbaric oxygen as an adjunct to acute revascularization of the brain. *Surg Neurol* 12:457–61

Kapp JP (1981) Neurological response to hyperbaric oxygen-—a criterion for cerebral revascularization. *Surg Neurol* 15:43–6

Khanna S, Roy S, Slivka A, Craft TK, Chaki S, Rink C, Notestine MA, DeVries AC, Parinandi NL, Sen CK (2005) Neuroprotective properties of the natural vitamin E alpha-tocotrienol. *Stroke* 36:2258–64

Kim GW, Kondo T, Noshita N, Chan PH (2002) Manganese superoxide dismutase deficiency exacerbates cerebral infarction after focal cerebral ischemia/reperfusion in mice: implications for the production and role of superoxide radicals. *Stroke* 33:809–15

Lambeth JD (2004) NOX enzymes and the biology of reactive oxygen. *Nat Rev Immunol* 4:181–9

Lau D, Baldus S (2006) Myeloperoxidase and its contributory role in inflammatory vascular disease. *Pharmacol Ther* 111:16–26

Lee ST, Chu K, Jung KH, Kim SJ, Kim DH, Kang KM, Hong NH, Kim JH, Ban JJ, Park HK, Kim SU, Park CG, Lee SK, Kim M, Roh JK (2008) Anti-inflammatory mechanism of intravascular neural stem cell transplantation in haemorrhagic stroke. *Brain* 131:616–29

Leonard EJ, Yoshimura T (1990) Human monocyte chemoattractant protein-1 (MCP-1). *Immunol Today* 11:97–101

Lou M, Eschenfelder CC, Herdegen T, Brecht S, Deuschl G (2004) Therapeutic window for use of hyperbaric oxygenation in focal transient ischemia in rats. *Stroke* 35:578–83

Loubinoux I, Volk A, Borredon J, Guirimand S, Tiffon B, Seylaz J, Meric P (1997) Spreading of vasogenic edema and cytotoxic edema assessed by quantitative diffusion and T2 magnetic resonance imaging. *Stroke* 28:419–26; discussion 426–417

Matsuo Y, Onodera H, Shiga Y, Nakamura M, Ninomiya M, Kihara T, Kogure K (1994) Correlation between myeloperoxidase-quantified neutrophil accumulation and ischemic brain injury in the rat. Effects of neutrophil depletion. *Stroke* 25:1469–75

Nemoto EM, Betterman K (2007) Basic physiology of hyperbaric oxygen in brain. *Neurol Res* 29:116–26

Nighoghossian N, Trouillas P, Adeleine P, Salord F (1995) Hyperbaric oxygen in the treatment of acute ischemic stroke. A double-blind pilot study. *Stroke* 26:1369–72

Paxinos G, Watson C (2005) *The Rat Brain in Stereotaxic Coordinates*. Amsterdam, Boston: Elsevier Academic Press

Price CJ, Menon DK, Peters AM, Ballinger JR, Barber RW, Balan KK, Lynch A, Xuereb JH, Fryer T, Guadagno JV, Warburton EA (2004) Cerebral neutrophil recruitment, histology, and outcome in acute ischemic stroke: an imaging-based study. *Stroke* 35:1659–64

Reglodi D, Tamas A, Lengvari I (2003) Examination of sensorimotor performance following middle cerebral artery occlusion in rats. *Brain Res Bull* 59:459–66

Reichel CA, Rehberg M, Lerchenberger M, Berberich N, Bihari P, Khandoga AG, Zahler S, Krombach F

(2009) Ccl2 and Ccl3 mediate neutrophil recruitment via induction of protein synthesis and generation of lipid mediators. *Arterioscler Thromb Vasc Biol* 29: 1787–93

Rha JH, Saver JL (2007) The impact of recanalization on ischemic stroke outcome: a meta-analysis. *Stroke* 38:967–73

Roy S, Khanna S, Kuhn DE, Rink C, Williams WT, Zweier JL, Sen CK (2006) Transcriptome analysis of the ischemia–reperfused remodeling myocardium: temporal changes in inflammation and extracellular matrix. *Physiol Genomics* 25:364–74

Roy S, Patel D, Khanna S, Gordillo GM, Biswas S, Friedman A, Sen CK (2007) Transcriptome-wide analysis of blood vessels laser captured from human skin and chronic wound-edge tissue. *Proc Natl Acad Sci USA* 104:14472–7

Rusyniak DE, Kirk MA, May JD, Kao LW, Brizendine EJ, Welch JL, Cordell WH, Alonso RJ (2003) Hyperbaric oxygen therapy in acute ischemic stroke: results of the Hyperbaric Oxygen in Acute Ischemic Stroke Trial Pilot Study. *Stroke* 34:571–4

Schmued LC, Hopkins KJ (2000) Fluoro-Jade B: a high affinity fluorescent marker for the localization of neuronal degeneration. *Brain Res* 874:123–30

Singhal AB (2007) A review of oxygen therapy in ischemic stroke. *Neurol Res* 29:173–83

Takizawa S, Aratani Y, Fukuyama N, Maeda N, Hirabayashi H, Koyama H, Shinohara Y, Nakazawa H (2002) Deficiency of myeloperoxidase increases infarct volume and nitrotyrosine formation in mouse brain. *J Cereb Blood Flow Metab* 22:50–4

Veltkamp R, Siebing DA, Heiland S, Schoenffeldt-Varas P, Veltkamp C, Schwaninger M, Schwab S (2005) Hyperbaric oxygen induces rapid protection against focal cerebral ischemia. *Brain Res* 1037:134–8

Vikram DS, Zweier JL, Kuppusamy P (2007) Methods for noninvasive imaging of tissue hypoxia. *Antioxid Redox Signal* 9:1745–56

Wang X, Feuerstein GZ, Gu JL, Lysko PG, Yue TL (1995) Interleukin-1 beta induces expression of adhesion molecules in human vascular smooth muscle cells and enhances adhesion of leukocytes to smooth muscle cells. *Atherosclerosis* 115:89–98

Weinstein PR, Anderson GG, Telles DA (1987) Results of hyperbaric oxygen therapy during temporary middle cerebral artery occlusion in unanesthetized cats. *Neurosurgery* 20:518–24

Wong CH, Crack PJ (2008) Modulation of neuroinflammation and vascular response by oxidative stress following cerebral ischemia–reperfusion injury. *Curr Med Chem* 15:1–14

Yamagami S, Tamura M, Hayashi M, Endo N, Tanabe H, Katsuura Y, Komoriya K (1999) Differential production of MCP-1 and cytokine-induced neutrophil chemoattractant in the ischemic brain after transient focal ischemia in rats. *J Leukoc Biol* 65:744–9

Yin D, Zhang JH (2005) Delayed and multiple hyperbaric oxygen treatments expand therapeutic window in rat focal cerebral ischemic model. *Neurocrit Care* 2:206–11

Supplementary Information accompanies the paper on the Journal of Cerebral Blood Flow & Metabolism website (http://www.nature.com/jcbfm)